

Switching Magnetization of a Nanoscale Ferromagnetic Particle Using Nonlocal Spin Injection

T. Kimura,^{1,2,3,*} Y. Otani,^{1,2,3} and J. Hamrle^{2,3}

¹*Institute for Solid State Physics, University of Tokyo, 5-1-5 Kashiwanoha, Kashiwa, Chiba 277-8581, Japan*

²*RIKEN FRS, 2-1 Hirosawa, Wako, Saitama 351-0198, Japan*

³*CREST, JST, Honcho 4-1-8, Kawaguchi, Saitama, 332-0012, Japan*

(Received 19 August 2005; published 23 January 2006)

We have performed nonlocal spin injection into a nanoscale ferromagnetic particle configured in a lateral spin-valve structure to switch its magnetization only by spin current. The nonlocal spin injection aligns the magnetization of the particle parallel to the magnetization of the spin injector. The spin current responsible for switching is estimated from the experiment to be about $200 \mu\text{A}$, which is reasonable compared with the values obtained for conventional pillar structures. Interestingly, the switching always occurs from antiparallel to parallel in the particle-injector magnetic configurations, where no opposite switching is observed. Possible reasons for this discrepancy are discussed.

DOI: [10.1103/PhysRevLett.96.037201](https://doi.org/10.1103/PhysRevLett.96.037201)

PACS numbers: 75.75.+a, 72.25.Ba, 72.25.Mk, 75.70.Cn

Spin-dependent transport properties have drawn enormous attention owing to the novel idea to utilize the spin angular momentum to operate future spintronic devices including a magnetic random access memory [1]. Unlike conventional inductive recording methods, the spin angular momentum transfer (*spin torque*) of conduction electrons is now employed to switch the magnetization. The current-induced magnetization reversal becomes one of the key technologies for developing spintronic devices. The switching mechanism due to spin torque is explained with models separately proposed by Berger [2] and Slonczewski [3] in which the torque exerted on the magnetization is proportional to the injected spin current. This clearly indicates that the spin current is essential to realize the magnetization switching due to the spin injection. Most of the present spin-transfer devices consist of vertical multilayered nanopillars in which, typically, two magnetic layers are separated by a nonmagnetic metal layer [4,5]. In such vertical structures, the charge current always flows together with the spin current, thereby undesirable Joule heat is generated. Our recent experiments have demonstrated that the spin currents are effectively absorbed into an additionally connected metallic wire with a small spin resistance [6,7]. This implies that the spin current without a charge flow can be selectively injected into a ferromagnetic particle with a small spin resistance, such as a Permalloy particle, replaced with the wire, and may contribute to the spin torque. To test this idea, a nanoscale ferromagnetic particle is configured for a lateral nonlocal spin-injection device as in Figs. 1(a) and 1(b).

The lateral multiterminal spin-injection device used for this study is fabricated on a thermally oxidized Si substrate by means of the conventional lift-off techniques. Figs. 1(c) and 1(d) show the scanning electron microscope (SEM) images of a fabricated device. The device consists of a large Permalloy (Py) pad 30 nm thick; a Cu cross 100 nm in width and 80 nm thick; and a Py nanoscale particle 50 nm in width, 180 nm in length, and 6 nm thick. A gold wire 100 nm in width and 40 nm thick is connected to the Py

particle to reduce the effective spin resistance, resulting in high spin-current absorption into the Py particle [6]. The magnetic field is applied along the easy axis of the Py particle. We note here that the dimensions of the Py pad and Cu wires are chosen to be large so that the charge current up to 15 mA can flow through them. The Py layer is grown using an electron beam evaporator with a base pressure of $2 \times 10^{-9} \text{ Torr}$. The Cu and Au wires are evaporated by a resistance heating evaporator with a base pressure of $3 \times 10^{-8} \text{ Torr}$. The interface between the Py and Cu and that between the Py and Au are well cleaned by Ar-ion milling prior to the Au and Cu depositions. Here the milling depth of the Py is less than 2 nm , and does not affect the magnetization switching behavior so much. Very

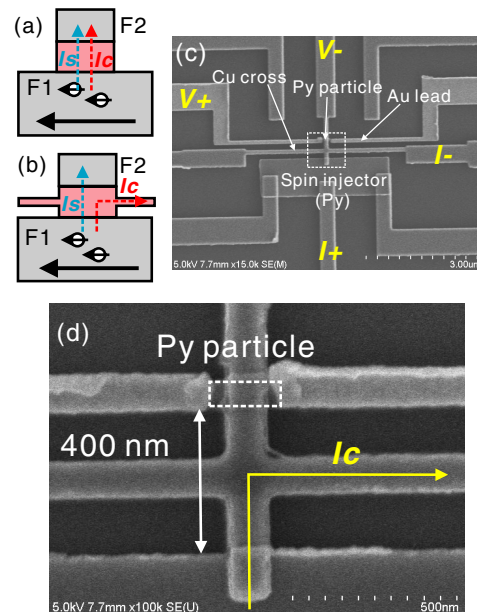


FIG. 1 (color online). Schematic illustrations of (a) the local spin injection and (b) nonlocal spin injection. (c) SEM image of the fabricated lateral spin-injection device and (d) magnified image around the Py particle.

low resistance of the interface assures good Ohmic contact. The distance between the Py pad and the particle is 400 nm. The resistivities of Py and Cu wires are respectively $10.2 \mu\Omega \text{ cm}$ and $1.14 \mu\Omega \text{ cm}$ at 77 K. The sample was cooled by immersing the sample holder directly into liquid nitrogen. All the measurements are performed at 77 K by using conventional lock-in technique.

Before showing the experimental results, we discuss spin-current absorption into the electrically floating additional wire. We have demonstrated that the spin-current distribution can be calculated by the model based on the spin-resistance circuit and that the spin current favors to flow in the subsection which has small spin resistance [6,7]. The spin resistance is given by $2\rho_i\lambda_i/(1-\alpha_i^2)S_i$, where ρ_i , λ_i , α_i , and S_i are the resistivity, spin diffusion length, spin polarization, and the cross section of the layer. For example, the spin resistance R_S^{Cu} for the Cu wire with the cross section of $100 \text{ nm} \times 80 \text{ nm}$ can be calculated as 4.28Ω . Here, we took the value of $1.5 \mu\text{m}$ for the spin diffusion length of Cu wire obtained in our experiments [8]. The effective cross section for the spin resistance of the Py particle in Fig. 1(d) is given by the junction area between the Py particle and the Cu wire because the spin diffusion length of the Py is quite short. Therefore, we obtain the spin resistance R_S^{Py} for the Py particle as 0.08Ω . Here, we use the spin polarization $\alpha_{\text{Py}} = 0.2$ and spin diffusion length $\lambda_{\text{Py}} = 2 \text{ nm}$ obtained in our experiments [8]. Important is that R_S^{Py} is about 2 orders of magnitude smaller than R_S^{Cu} . Thus, when the spin current reaches the junction between the Py particle and the Cu wire, the spin current favors being absorbed into the Py particle although the particle is electrically floating. Such an absorption can be employed as a method to inject the spin current nonlocally.

To begin with, the nonlocal spin-valve (NLSV) measurements are performed to understand the spin accumulation behaviors in our devices [9]. Figure 2(a) shows the NLSV signal with the inset of the measurement probe configuration. We can see a clear spin signal of $0.18 \text{ m}\Omega$. Here, the resistance changes at low and high fields correspond to the relative magnetic switching of the Py pad and particle, from parallel (P) to antiparallel (AP) states and *vice versa*. These results prove that the spin current from the Py pad is absorbed into the Py particle. It should be noted that the measured spin signal is smaller than the value expected from our previous experiments [6–8]. As will be mentioned later, this is because the Py particle used in the present study has smaller spin resistance than the values estimated from our lateral spin-valve experiments.

Then, we examine the effect of the nonlocal spin injection into the Py particle with using the same probe configuration. Before performing the nonlocal spin injection, the magnetization configuration is set in the AP configuration by controlling the external magnetic field. The nonlocal spin injection is performed by applying large pulsed

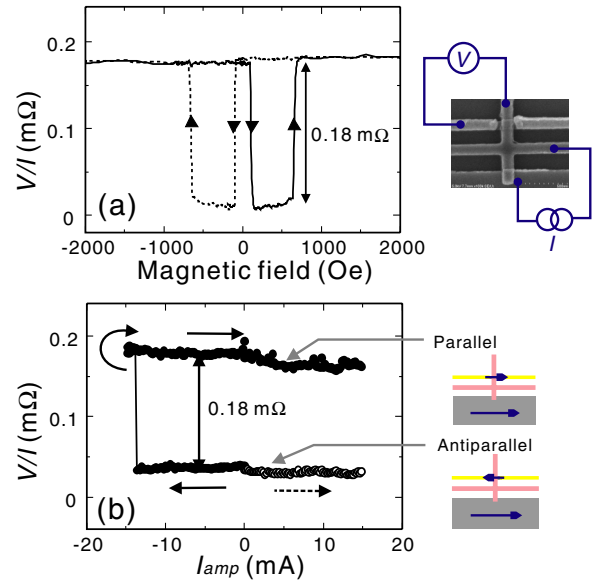


FIG. 2 (color online). (a) Nonlocal spin-valve signal with the probe configuration. The solid and dotted lines correspond to the positive and negative field sweep, respectively. (b) The NLSV signal after the pulsed current injection as a function of the current amplitude with the corresponding magnetization configurations.

currents up to 15 mA with the same current probes for the NLSV measurement in the absence of magnetic field. Note that the current pulse is triangular shape with the period of 1 s. After the nonlocal spin injection, the NLSV signal is successively measured to determine the magnetic state of the Py particle. In this way, as shown in Fig. 2(b), the NLSV signal after the nonlocal spin injection, as a function of the amplitude of the pulsed current, is obtained. When the magnitude of the pulsed current is increased positively in the AP state, no signal change is observed up to 15 mA. On the other hand, for the negative scan, the abrupt signal change is observed at -14 mA . The change in resistance at -14 mA is $0.18 \text{ m}\Omega$, corresponding to that of the transition from AP to P states. The magnetization direction of the Py particle is confirmed to be parallel to the Py pad by sweeping the magnetic field with measuring the NLSV signal. After the transition from the AP to P states, the current is positively increased in the P state. However, we observe no signal change even though the amplitude of the pulsed current was increased up to 15 mA. In this measurement, there are 2 equivalent AP states in which the magnetization of the Py particle directs towards either left or right in Fig. 2(b). Both AP states are found to transform to the P state in the same manner. We can exclude as follows a possibility that the magnetization of the Py particle is switched by the current-induced Oersted field. In the probe configuration for the nonspin injection, the charge current passes through the Cu cross and induces the Oersted field. However, the induced field is normal to the substrate and thus does not switch the magnetization of the

Py particle since the demagnetizing field of nearly 1 T is far bigger than the Oersted field.

Figure 3(a) shows the similar measurement performed with the different probe configuration in the inset. We also obtain a clear spin signal of 0.19 mΩ, slightly larger than that in the previous configuration. The difference in the magnitude of the spin signal from the previous probe configuration is understood by the inhomogeneous spin-current distribution [10]. Then, the similar spin-injection measurements are performed. Figure 3(b) shows the NLSV signal after the nonlocal spin injection as a function of the amplitude of the pulsed current. The clear transition from the AP to P states is observed whereas the reverse P to AP transition is not observed. In this case, the switching occurs at -13.3 mA slightly smaller than that in the previous probe configuration. This is because the larger spin accumulation at the interface induces the larger spin current than in the previous configuration. In this probe configuration, the distribution of the Oersted field is different from the previous experiment. No remarkable difference in the transition behaviors between Figs. 2 and 3 supports that the observed AP to P transition is not originated by the Oersted field. We like to point here that for both cases the Oersted field exerted normal to the substrate causes a deviation from the collinear magnetic configuration between Py pad and particle [11], and may assist the magnetization switching of the Py particle due to the spin torque, leading to the reduction of the switching current.

We estimate the magnitude of injected spin current into the Py particle in the AP state. When the electrons are

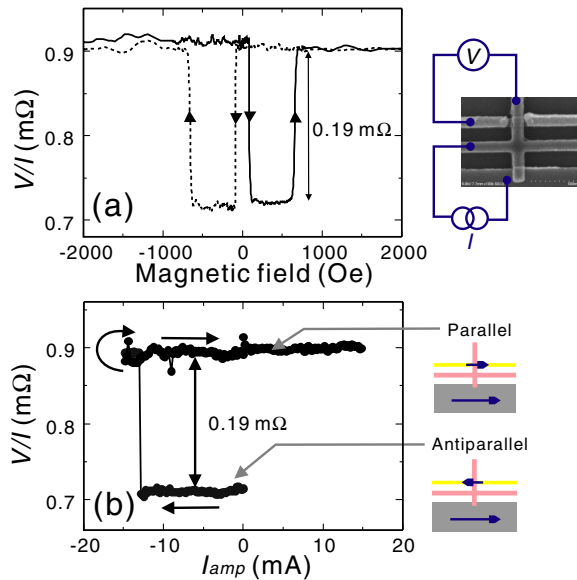


FIG. 3 (color online). (a) Nonlocal spin-valve signal with the probe configuration. The solid and dotted lines correspond to the positive and negative field sweep, respectively. (b) The NLSV signal after the pulsed current injection as a function of the current amplitude with the corresponding magnetization configurations.

injected from the Py pad into the Cu wire (negative current), the Cu wire is magnetized in parallel to the Py pad due to the spin accumulation. The continuity of the chemical potential at the interface also brings about the spin splitting in the Py particle, as shown in Figs. 4(a) and 4(c). The spin-dependent chemical potential of the Py particle in antiparallel to the Py pad is given by [12]

$$\mu_{\uparrow} = \mu_i \left(\frac{\alpha_{\text{Py}}}{2} - \frac{1 + \alpha_{\text{Py}}}{2} e^{-x/\lambda_{\text{Py}}} \right), \quad (1)$$

$$\mu_{\downarrow} = \mu_i \left(\frac{\alpha_{\text{Py}}}{2} + \frac{1 - \alpha_{\text{Py}}}{2} e^{-x/\lambda_{\text{Py}}} \right). \quad (2)$$

Defining the spin current as $I_S = I_{\uparrow} - I_{\downarrow} = -(S_{\text{Py}}\sigma_{\uparrow}/e) \times (\partial\mu_{\uparrow}/\partial x) + (S_{\text{Py}}\sigma_{\downarrow}/e) (\partial\mu_{\downarrow}/\partial x)$ yields the injected (absorbed) total spin current into the Py particle:

$$I_S = \frac{\sigma_{\text{Py}} S}{e} \left(\frac{(1 - \alpha_{\text{Py}})}{2} \frac{\partial\mu_{\uparrow}}{\partial x} \Big|_{x=0} - \frac{(1 + \alpha_{\text{Py}})}{2} \frac{\partial\mu_{\downarrow}}{\partial x} \Big|_{x=0} \right) \quad (3)$$

$$= \frac{(1 - \alpha_{\text{Py}}^2) \sigma_{\text{Py}} S}{2e\lambda_{\text{Py}}} \mu_i = \frac{\mu_i}{eR_S^{\text{Py}}}. \quad (4)$$

This means that in the AP states the spin current along the Py pad is injected into the Py particle. This discussion also stands for the P configuration as in Fig. 4(c). Therefore, the spin current induced by nonlocal spin injection with the negative current injection aligns the magnetization of the Py particle along the Py pad. The magnitude of the injected spin current can be deduced from the intensity of the spin signal by using Eq. (4). The relation between the induced spin splitting in the chemical potential μ_i at the interface and the obtained spin signal R_{NLSV} in the NLSV measure-

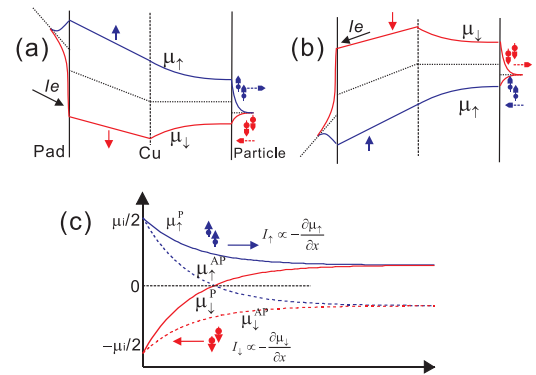


FIG. 4 (color online). Schematic illustrations of (a) the induced chemical potential with the negative current injection in the antiparallel configuration and (b) that with the positive current injection in the parallel configuration. (c) Spin-dependent chemical potential inside of the Py particle in parallel (antiparallel) to the Py pad in the negative current. The direction of the injected spin current depends on the polarity of the current and does not depend on the magnetization configuration between the Py pad and the Py particle.

ment is given by $\mu_i = e i_c R_{\text{NLSV}} / \alpha_{\text{Py}}$. Here, i_c is the exciting charge current for the measurement. Therefore, when we inject a pulsed current with an amplitude of I_{amp} , the injected spin current I_{Sinj} into the Py particle can be calculated as

$$I_{\text{Sinj}} = \frac{\mu_i}{e R_S^{\text{Py}}} = \frac{R_{\text{NLSV}} I_{\text{amp}}}{\alpha_{\text{Py}} R_S^{\text{Py}}}. \quad (5)$$

As mentioned above, the spinresistance of the Py particle is 0.08Ω . When we use the parameters determined in previous experiments [8], we obtain the injected spin current as $158 \mu\text{A}$ for $I_{\text{amp}} = 14 \text{ mA}$. The value can be compared with that of conventional pillar structures consisting of Py-based current perpendicular to plane devices [13,14]. The observed spin current for switching the free layer from the AP to P state in the vertical structures ranges typically about $200 \mu\text{A}$ that are comparable to our present experiment. As mentioned above, the obtained spin signal is smaller than that in the NLSV experiment with the same injector-detector distance. We believe that this is caused by the lower quality of the Py particle than the Py element in our previous lateral spin-valve experiments. In the Py particle, the effect of the surface oxidation is more pronounced than the conventional devices because of the small sample dimensions. Such effects reduce the spin polarization and the spin diffusion length of the Py particle. This causes the reduction of the spin resistance and thus lowers the estimation of the spin splitting voltage at the interface. The real injected spin current may thus be larger than the above calculation.

Similar analysis for the positive current results in the spin current with the same magnitude and the opposite polarity injected into the Py particle as in Fig. 4(b). Therefore, the spin current induced by nonlocal spin injection with the positive current leads the Py particle magnetization into the AP state. This transition, however, is not observed in the present experiment. Although the concrete reason has not been clarified yet. Conceivable explanations for this discrepancy may be as follows. One is a bias dependent spin polarization of the Py pad. In general, the spin polarization should be independent of the current passing through the interface in the Ohmic junction. However, it is not true once a very thin oxide layer is formed at the interface between the Py pad and Cu cross during the fabrication process. Note that our device is exposed to the air during the process. Such an oxidized layer may provide an asymmetric barrier especially at high current density. Therefore, we have to take into account an asymmetric spin injection into or out of the Py pad. When the electron is injected from the Cu wire into the Py pad, the spin polarization drastically reduces compared to the zero bias value with increasing the applied bias voltage [15], thus diminishing the injected spin current into the Py

particle. On the contrary, the spin polarization exhibits only a small reduction when the electron is injected from the Py pad into the Cu wire. In this way, our asymmetric reversal of the Py nanoparticle can be explained. Another possibility is a tiny magnetic impurity in the Cu wire near the interface. The spin diffusion length of the Cu wire with the magnetic impurity is known to depend on the angle between the direction of the impurity magnetic moment and that of the injected spin [16]. When the direction of the injected spin is antiparallel to the moment of the magnetic impurity, the spin diffusion length is shorter than that at the parallel alignment because of the reorientation of the magnetic moment of the conduction electron spin to the direction of that of the magnetic impurity. The magnetic impurity in the Cu wire may be parallel to the magnetization of the Py pad because of the exchange interaction. In this case, when the electron is injected from the Cu wire to the Py pad (corresponding to the positive current), the spin diffusion length is shorter than that of the negative current. This asymmetric transport also explains our experimental results.

In summary, we succeeded in switching the magnetization of the Py particle from the AP to the P states by nonlocal spin injection. However we could not realize the P to AP switching by changing the polarity of the pulsed exciting current. The value of the switching spin current obtained from the experiment was reasonable compared with the values estimated from the conventional pillar devices. In order to realize both switchings of the Py particle, further optimization of the device structure is required.

*Electronic address: kimura@issp.u-tokyo.ac.jp

- [1] S. A. Wolf *et al.*, *Science* **294**, 1488 (2001).
- [2] L. Berger, *Phys. Rev. B* **54**, 9353 (1996).
- [3] J. C. Slonczewski, *J. Magn. Magn. Mater.* **159**, L1 (1996).
- [4] M. Tsoi *et al.*, *Phys. Rev. Lett.* **80**, 4281 (1998).
- [5] F. J. Albert *et al.*, *Phys. Rev. Lett.* **89**, 226802 (2002).
- [6] T. Kimura, J. Hamrle, and Y. Otani, *Phys. Rev. B* **72**, 014461 (2005).
- [7] T. Kimura *et al.*, *Appl. Phys. Lett.* **85**, 3795 (2004).
- [8] T. Kimura, J. Hamrle, and Y. Otani (unpublished).
- [9] F. J. Jedema, A. T. Filip, and B. J. van Wees, *Nature (London)* **410**, 345 (2001);
- [10] T. Kimura *et al.*, *J. Magn. Magn. Mater.* **286**, 88 (2005).
- [11] B. Oezylmaz *et al.*, *Phys. Rev. Lett.* **91**, 067203 (2003).
- [12] S. Takahashi and S. Maekawa, *Phys. Rev. B* **67**, 052409 (2003).
- [13] I. N. Krivorotov *et al.*, *Science* **307**, 228 (2005).
- [14] S. Urazhdin *et al.*, *Phys. Rev. Lett.* **91**, 146803 (2003).
- [15] S. O. Valenzuela *et al.*, *Phys. Rev. Lett.* **94**, 196601 (2005).
- [16] C. Heide, *Phys. Rev. B* **65**, 054401 (2002).